Phase Behavior of Model Lipid Systems: Solubility of High-Melting Fats in Low-Melting Fats

Yuqing Zhou and Richard W. Hartel*

Department of Food Science, University of Wisconsin–Madison, Madison, Wisconsin 53706

ABSTRACT: The solubility behavior of three high-melting fats (tripalmitin sample, PPP-S; cocoa butter-stearin, CB-S; and palm oil-stearin, PO-S) in five low-melting fats (tricaprylin, CCC; canola oil; sunflower oil; lard-olein, LD-O; and palm oil-olein, PO-O) was studied. To create the solubility curve, the high-melting fat was first equilibrated in the low-melting model lipid system between 25 and 62.5°C for 1 wk. The amount of high-melting fat dissolved in the low-melting model lipid system was then determined by analyzing TAG compositions in the liquid phase using GC. The low-melting CCC formed partial solid solutions with each of the high-melting fats as a result of its very short chain length. PPP-S formed an ideal solution in all of the low-melting fats except CCC. The mixtures of CB-S/LD-O, CB-S/PO-O, and PO-S/LD-O deviated from ideality, illustrating closer interactions between TAG from CB-S and PO-S and those from LD-O or PO-O. The melting temperature and heat of fusion of the high-melting fats calculated from the Hildebrand equation was very close to those determined by DSC.

Paper no. J11292 in *JAOCS 83*, 505–511 (June 2006).

KEY WORDS: Heat of fusion, Hildebrand equation, ideal solution, lipids, melting temperature, solubility.

In food products, it is common to find that high-melting and low-melting fats have been included for their specific appearance, texture, and mouthfeel attributes. For example, one option in the production of soft and spreadable butter is to combine 70–80% very low melting milk fat fraction with 20–30% high-melting milk fat fraction (1). The softening effect of low-melting fat is, in part, due to the dissolution of high-melting components (solute) into the liquid components (solvent). In addition, the solubility of the high-melting component also directly relates to the crystallization kinetics. Therefore, it is important to understand the mixing behavior of high-melting fats in low-melting oils.

The solubility of a high-melting fat is best described through a solubility curve, which, as part of the complete phase diagram, depicts the equilibrium relationship between temperature and composition of high-melting component (solute) in the liquid oil (solvent). Although various researchers have studied the phase behavior of pure TAG, very few studies have been done on the solubility of natural fats, largely due to the complex composition. Hannewijk *et al*. (2) presented some results on the solubility of fully hardened groundnut oil in linseed oil determined by using dilatometry. Timms (3) studied the solubility of milk fat, fully hardened milk fat, and milk fat hard fraction in liquid oils by determining the softening point of the mixtures when heated in a differential scanning calorimeter (DSC).

In most cases, the equilibrium relationship of pure TAG mixtures is determined by measuring its m.p. However, there is no single m.p. for natural fats since they are made up of a number of different TAG. Many methods can be used to determine the melting temperature, such as the clear point, softening point, slip point, or Wiley m.p. (4). Consequently, the "solubility" of natural fats, as measured by thermal methods, depends to some extent on how the melting temperature is measured.

When one assumes solution behavior rather than melt behavior, solubility is typically measured by using a compositional approach (5). Actually, a dual approach is preferred to ensure that equilibrium is attained from both directions—dissolution and crystallization. In one case, excess crystalline phase is added to the solvent at a given temperature and solute allowed to dissolve to equilibrium. In the other case, a supersaturated solution is created at the same temperature and crystallization is allowed to occur until equilibrium is attained. In both cases, the solubility is measured by analyzing the amount of solute found in the solvent at equilibrium. Both methods should give the same solubility if true equilibrium has been reached.

Another method of characterizing the equilibrium condition between crystalline and liquid fat is the point of zero solid fat as measured by pulsed NMR. Although NMR is typically used to characterize the entire melting profile, or solid fat content (SFC) curve, of a fat, the temperature at which the SFC goes to zero also may be used to indicate the equilibrium condition.

Many TAG mixtures form an ideal solution in the liquid state (6), and the solubility of high-melting saturated TAG in the low-melting unsaturated TAG follows the Hildebrand equation (7), i.e., Equation 1:

$$\ln x = -\frac{\Delta H_{fus}}{R}\left(\frac{1}{T} - \frac{1}{T_0}\right) \qquad [1]$$

where x = solubility of high-melting component (mol/mol), ΔH_{fus} = heat of fusion of high-melting component (kJ/mol), T_0 = melting temperature of high-melting component (K), T = experimental temperature (K), and R = gas constant (kJ/mol·K).

The Hildebrand equation assumes that the high-melting component forms an ideal solution with the low-melting component, so the type of low-melting component has no effect on

*To whom correspondence should be addressed. E-mail: rwhartel@wisc.edu

the solubility of high-melting component. However, natural fats contain a wide range of TAG compositions, and the interactions among these TAG may lead to deviations from ideal solution behavior.

This study was designed to use model binary lipid systems with relatively narrow ranges of TAG composition to study phase behavior using a compositional analysis method. Mixtures of the model lipids were equilibrated, and the composition in the liquid phase was analyzed by GC. The results were used to construct the partial solubility lines, which then were compared with results from thermal analysis (DSC) and SFC (NMR).

EXPERIMENTAL PROCEDURES

Materials. In this study, the model lipids (three high-melting fats and five low-melting fats) were obtained either by purchasing directly from the manufacturer or by fractionating natural fats (Table 1). The high-melting fats were tripalmitin sample (PPP-S, >85% purity; Sigma Chemical Co., St. Louis, MO), cocoa butter-stearin (CB-S; Lyons & Sons Co., NJ), and palm oil-stearin (PO-S; Cargill, Minneapolis, MN). The low-melting fats included tricaprylin (CCC, >99%purity; Sigma Chemical Co.), canola oil (CNO; Cargill), sunflower oil (SFO; Cargill), lard-olein (LD-O; Bunge Foods, St. Louis, MO), and palm oil-olein (PO-O; Cargill).

TAG analysis. TAG composition, analyzed by GC, is often reported based on the carbon number (CN) of the TAG (i.e., saturated and unsaturated TAG with the same CN were eluted together). In some circumstances, finer resolution of TAG composition is needed. Geeraert and Sandra (7) were able to resolve TAG in chocolate fats according to the number of unsaturated FA using a capillary column with a polar stationary phase. In their case, the retention time increased with increasing number of double bonds (e.g., OOO > StOO > StOSt > StStSt, where O = oleate and St = stearate).

In this study, TAG analysis of the model lipid systems was determined by using a Hewlett-Packard 5890 Series II (Agilent, Palo Alto, CA) GC unit equipped with an FID and on-column injector. The column used was a 30-m long Heliflex Phase AT-1 having an i.d. of 0.25 mm (Alltech Associates, Deerfield, IL). Helium was the carrier gas at a flow rate of 2 mL/min with hydrogen gas and air also being supplied to the FID.

Between 4 and 15 mg of the model lipid systems was weighed out in GC vials (Alltech) and dissolved in 1.5 mL of 2,2,4-trimethylpentane. The internal standard was 100 μL trinonanoin at a concentration of 202 μg trinonanoin/μL of 2,2,4-trimethylpentane. A 5-μL sample of this solution was injected through an on-column injector. The TAG composition was determined using the following temperature program: initial hold at 220°C for 1 min; increase to 260°C at a rate of 2.0°C/min; then increase the temperature to 300°C at a rate of 1.2°C/min and hold for 10 min; increase to 329°C at 0.8°C/min and hold for 45 min. The total run time was 145.6 min. The pressure and the detector temperature were held constant at 20 psi (138 kPa) and 340°C, respectively. With this program, the retention time decreased as the number of double bonds in the TAG (i.e., OOO < StOO < StOSt < StStSt) increased. The composition was based on the area percentage of peaks collected and integrated using ChemStation chromatography software by Agilent. The average of three measurements was calculated.

Table 1 lists the TAG composition of each sample. Although the goal was to define model lipids with a narrow range of TAG within a given compositional type, it is apparent that each fat sample contained a range of components. The first two high-melting fats, PPP-S and CB-S, each contained several TAG; however, all of the TAG in each sample were within the same category. That is, PPP-S contained all-trisaturated TAG, whereas CB-S contained all monounsaturated TAG with the unsaturated FA in the *sn*-2 position. The third high-melting fat, PO-S, contained a wider range of TAG in several different classes of unsaturation. Likewise, the low-melting fats, with the exception of the pure CCC, contained a relatively wide range of TAG that overlapped several differ-

TABLE 1
Classes of Model Lipids with TAG Classification

	Abbreviation	Description	Composition[a]
High-melting fats	PPP-S	Tripalmitin sample (>85% purity)	PPP (84.9%); PPS (10.6%); MPP (3.2%)
	CB-S	Second-stage solid fraction (stearin) from cocoa butter	SOP (40.1%); SOS (36.6%); POP (19.2%)
	PO-S	First-stage solid fraction (stearin) from palm oil	POP (38.3%); OOP (16.2%); PPP (26.9%); PPS (3.4%); SOP (3.8%); MPP (2.1%); OOS + SOS (5.3%)
Low-melting fats	PO-O	Second-stage liquid fraction (olein) of palm oil	POP (37.1%); OOP (37.1%); SOP (3.6%); OOS + SSO + SSS (13.4%)
	LD-O	Fifth-stage liquid fraction (olein) from lard	OOP (48.2%); POP (11.0%); PPS (4.0%); SOP (4.2%); OOO + LLL (16.2%); OOS + SSO + SSS (12.6%)
	CNO	Canola oil	OOO + LLL (77.5%); SOP (12.5%); SOO (6.9%)
	SFO	Sunflower oil	OOO + LLL (74.4%); OOP (15.1%); SOO (7.1%)
	CCC	Tricaprylin (>99% purity)	CCC (100%)

[a]P, palmitic acid; O, oleic acid; S, stearic acid; M, myristic acid; L, linoleic acid; C, caprylic acid; PPP-S, tripalmitin sample; CB-S, cocoa butter stearin; PO-S, palm oil stearin; PO-O, palm oil olein; LD-O, lard olein.

ent classes. No further attempts to narrow the range of TAG were performed.

Melting profile. Melting point and ΔH_{fus} of model lipid systems were determined using a PerkinElmer DSC-7. The model lipid systems were stored at −20°C for at least 3 mon to ensure formation of the most stable polymorph. The instrument was calibrated with mercury and indium standards. Between 6 and 10 mg of fats was heated from −50 to 80°C at 5°C/min. Onset, peak, and end temperatures were recorded. Total area under the melting curve was calculated as ΔH_{fus}. The average of at least three measurements was calculated.

SFC. The SFC of mixtures of each of the model lipid systems was measured with a Bruker Minispec 120 NMR spectrometer (Bruker, Ontario, Canada) operating at a field strength of 0.47 Tesla, and equipped with Minispec software (PC-Control 232). The instrument measured the magnetization signal from both solid and liquid using the direct method after calibration with 0, 30, and 70% SFC standards. Samples were melted at 80°C for 30 min, filled into 10-mm (diameter) NMR tubes, and tempered according to the IUPAC method 2.150 (8). Tempering consisted of holding samples at 80°C for 20 min, quenching to 0°C for 90 min, holding at 26°C for 40 h, and finally, holding at 0°C for 90 min before taking the SFC measurement. Readings were taken as temperature was increased in 5°C increments (sometimes 2.5°C increments when needed) until melting. Each sample was prepared in triplicate and the average SFC calculated.

The temperature at which the SFC went to zero was taken as a measure of the equilibrium condition for each mixture. Since NMR readings are notoriously inaccurate at SFC levels of a few percent, the temperature at which SFC was zero was estimated by interpolation from the last three points according to the method of Timms (9) during construction of isosolid diagrams (10).

Determination of solubility curve. To determine the solubility of the most stable polymorph of the high-melting fat in the low-melting oils at each temperature, the fully crystallized solid fat (most stable polymorph) was allowed to dissolve in the liquid oil (the low-melting fat remained liquid at the experimental temperatures) with good agitation for a week to ensure equilibration. Equilibration after 1 wk was confirmed by repeated compositional analysis for up to 3 wk of mixing at the lowest temperature studied for each high-melting fat. The temperature range was governed by the m.p. of the high-melting fat. For the PPP-S sample, the lowest temperature studied was 45°C, whereas the lowest temperature studied for the CB-S and PO-S samples was 25°C. After 1 wk of agitation at each temperature of study, the solid and liquid phases were separated through vacuum filtration, and the amount of high-melting fat dissolved in the low-melting fat was determined by analyzing permeate composition with GC. The solubility of high-melting fat was determined by adding the peak areas from all the TAG in the high-melting fat and dividing by the total area of TAG in the GC sample. In the case of the PPP-S sample, the solubility of the PPP molecule was also obtained.Triplicate measurements were done for each analysis.

RESULTS AND DISCUSSION

Melting behavior. The melting temperature of a fat can be determined by numerous methods, such as clear-point, softening-point, and slip-point. Often, people use DSC to determine the melting behavior of a fat due to its convenience and speed. One should be aware that fats containing multiple TAG often exhibit multiple peaks or a single peak in a less stable polymorph in a DSC profile. Therefore, the melting temperature and ΔH_{fus} determined from the melting profile of a fat should be used with care.

The melting temperature and ΔH_{fus} of each model lipid system, as measured by DSC analysis, are shown in Table 2. The three high-melting fats (CCC, PPP-S, and CB-S) generally melted within a very narrow temperature range, in line with their composition. CCC had very high purity, and its melting range between end temperature and onset temperature was only about 3.4°C. All three high-melting fats (PPP-S, CB-S, and PO-S) exhibited a single melting peak, although the melting range of PO-S was broad. In this study, PPP-S, CB-S, and PO-S were believed to reach the most stable polymorph; it is therefore acceptable to use peak or end temperature as their melting temperatures. In general, the more complex the TAG composition, the broader the melting ranges were.

On average, PPP-S had the highest ΔH_{fus} and SFO had the lowest, as expected from the nature of the TAG in each model lipid system. Lipids with long-chain saturated TAG (such as

TABLE 2
Melting Parameters for the Model Lipid Systems Measured by DSC[a]

Model lipid systems	Onset temperature (°C)	End temperature (°C)	Peak temperature (°C)	ΔH_{fus} (kJ/mol)
PPP-S	60.6 ± 0.1	64.7 ± 0.2	63.4 ± 0.2	150.5 ± 10.7
CB-S	34.4 ± 0.4	38.1 ± 0.8	36.5 ± 0.8	119.4 ± 9.6
PO-S	3.5 ± 0.4	57.1 ± 0.2	54.9 ± 0.4	73.9 ± 5.4
CCC	7.4 ± 0.2	10.8 ± 0.6	9.9 ± 0.2	41.2 ± 7.2
SFO	−32.2 ± 0.6	−26.9 ± 0.9	−29.3 ± 0.7	39.6 ± 7.8
CNO	−26.5 ± 0.5	−8.1 ± 0.4	−17.0 ± 0.2	41.0 ± 12.1
LD-O	−11 ± 0.2	20.4 ± 0.5	4.6 ± 0.2	49.4 ± 4.2
PO-O	−7.1 ± 0.4	22.1 ± 0.8	3.8 ± 0.5	45.2 ± 11.9

[a]The samples were heated from −50 to 80°C at 5°C/min. For abbreviations see Table 1.

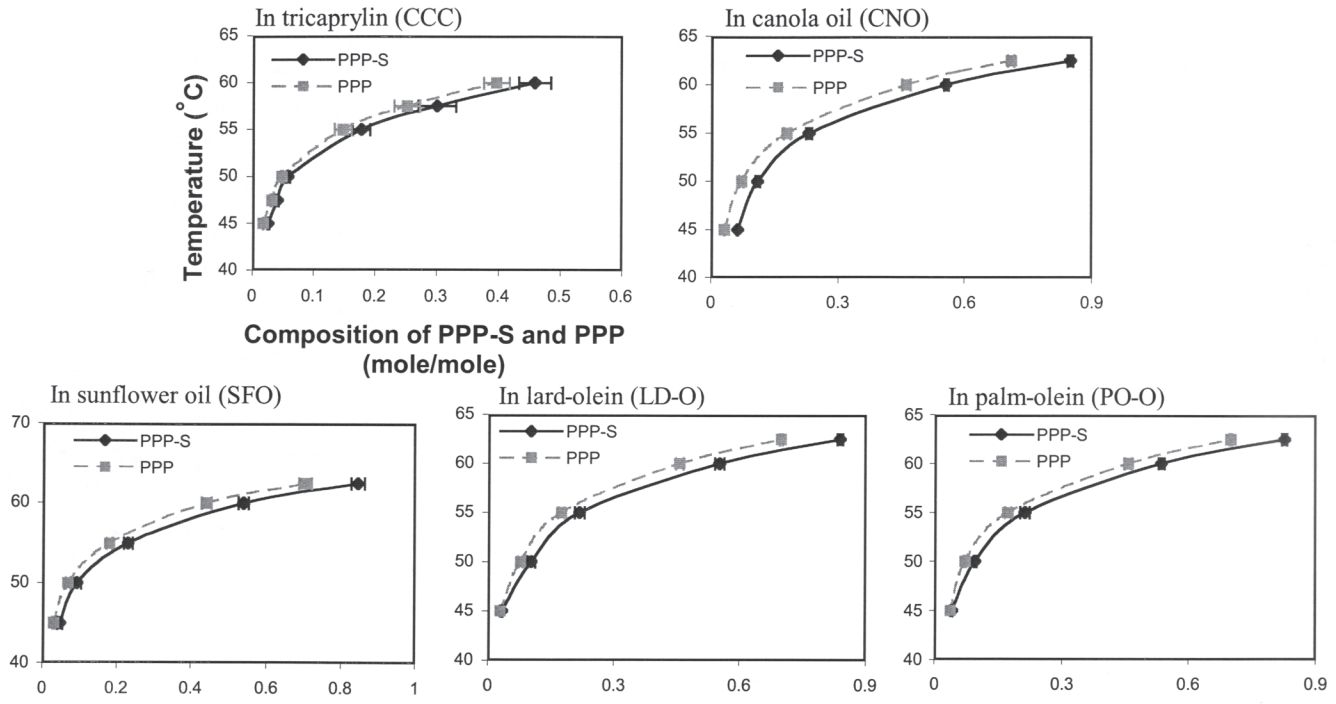

FIG. 1. Solubility, expressed as a mole fraction (x) of tripalimitin sample (PPP-S), and its main component, tripalmitin (PPP) in several low-melting fats as solvent.

PPP-S) had much higher ΔH_{fus} values than those composed mainly of short-chain or unsaturated TAG.

Solubility. According to the Hildebrand equation, the relationship between solubility and temperature is often illustrated in the plot of ln(x) vs. 1/T, where x is the solubility (mole fraction) of high-melting fat and T is the temperature at which the solubility is measured. If a linear relationship between ln(x) and 1/T is found, the system may exhibit ideal mixing behavior, and the melting temperature of high-melting fat can be calculated.

(i) PPP-S. Figure 1 shows the solubility curve of PPP-S and its main component, PPP, in five low-melting fats in the range from 45 to 62.5°C. As expected, the overall solubility of PPP-S is dominated by the solubility of its main component, PPP, since the solubility of PPP is nearly identical to that of the slightly less pure sample, PPP-S. As the temperature was increased, the solubility or concentration of PPP-S increased. This same general trend was seen for all samples studied.

The log value of the solubility of PPP-S had a linear relationship with 1/T, as seen in Figure 2 (solid lines), which indicated that PPP-S might form an ideal solution with each of the low-melting fats. However, if a true ideal solution did form between PPP-S and the low-melting fats, then the solubility of PPP-S would be the same in these low-melting fats. To confirm ideality, the results for the solubility of PPP-S in all low-melting fats were compared and analyzed by ANOVA (data not shown). The statistical results indicated that the solubility of PPP-S was the same in CNO, SFO, LD-O, and PO-O ($P <$ 0.05), especially when the temperature was higher than 50°C, which indicated that these low-melting fats had no effect on the dissolution of PPP-S. However, the solubility of PPP-S in CCC was consistently lower than in the other fats. The lower-than-ideal solubility was explained by Knoester *et al.* (11) as being due to formation of a solid solution between high-melting and low-melting components.

(ii) CB-S. The solubility of CB-S in the low-melting fats is shown in Figure 3 (solid lines). A linear relationship is found in the systems of CB-S/CCC, CB-S/CNO, and CB-S/SFO. However, the other two binary mixtures, CB-S/LD-O and CB/PO-O, showed nonlinear relationships.

For the determination of whether CB-S formed an ideal solution with the low-melting fats, results of the solubility of CB-S in the various low-melting fats were compared. The solubility of CB-S in CNO and in SFO was the same between 25 and 32.5°C (confirmed by ANOVA analysis), and the log value of the solubility of CB-S was linearly related to 1/T (Fig. 3), which indicated an ideal solution in these two binary systems. However, the solubility of CB-S in CCC, LD-O, and PO-O was significantly lower than in CNO and SFO.

The low solubility of CB-S in CCC, LD-O, and PO-O implied that a solid solution formed between CB-S and CCC, LD-O, or PO-O. This cocrystallization of low-melting fats in CB-S reduced the solubility of CB-S.

(iii) PO-S. When the solubility of PO-S in various low-melting fats was plotted against 1/T, a straight line was obtained with all the low-melting fats except LD-O (Fig. 4). Statistical analysis (ANOVA) showed that the results of the solubility of PO-S in CNO, SFO, and PO-O were identical ($P < 0.05$) at all temperatures (30–50°C), which indicated an ideal solution in

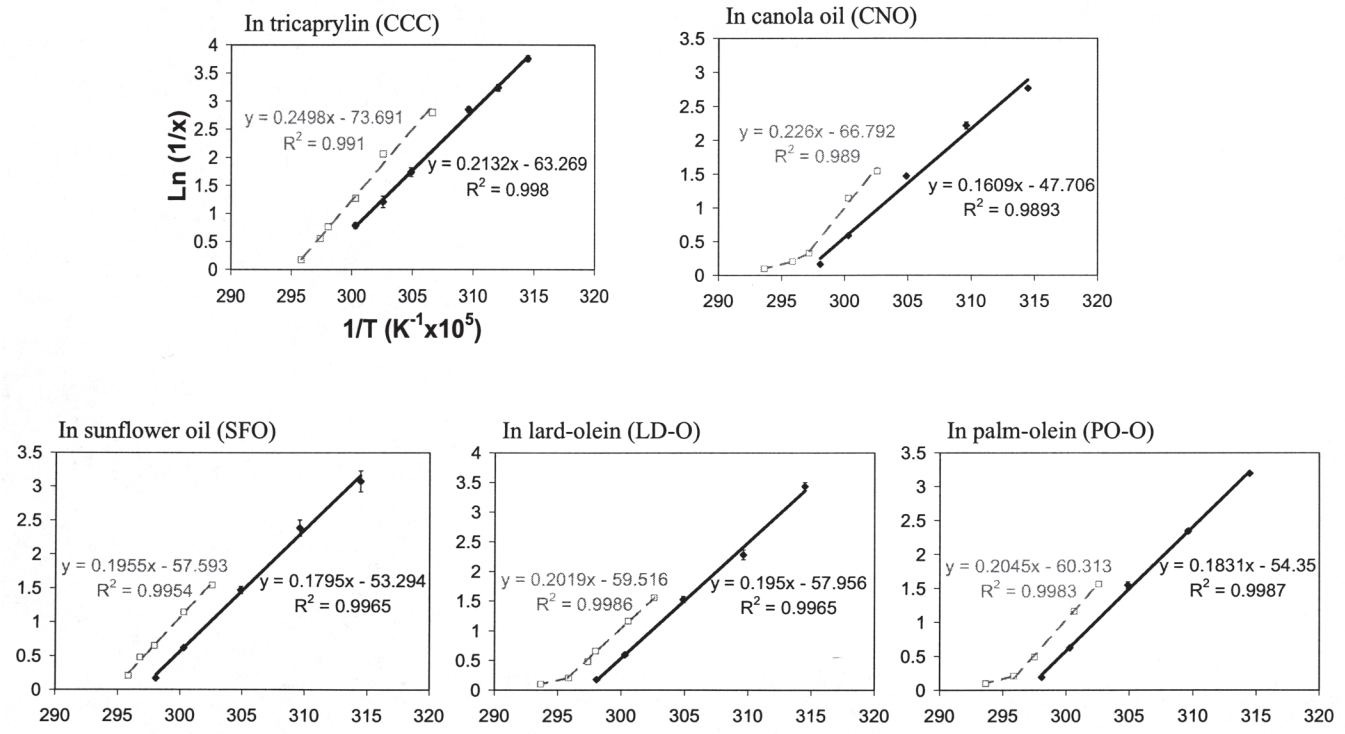

FIG. 2. Solubility curve (*x*, mole fraction) of tripalmitin sample (PPP-S), as measured by compositional analysis (◆, solid lines) and extrapolated 0% solid fat measured by NMR (□, dashed lines).

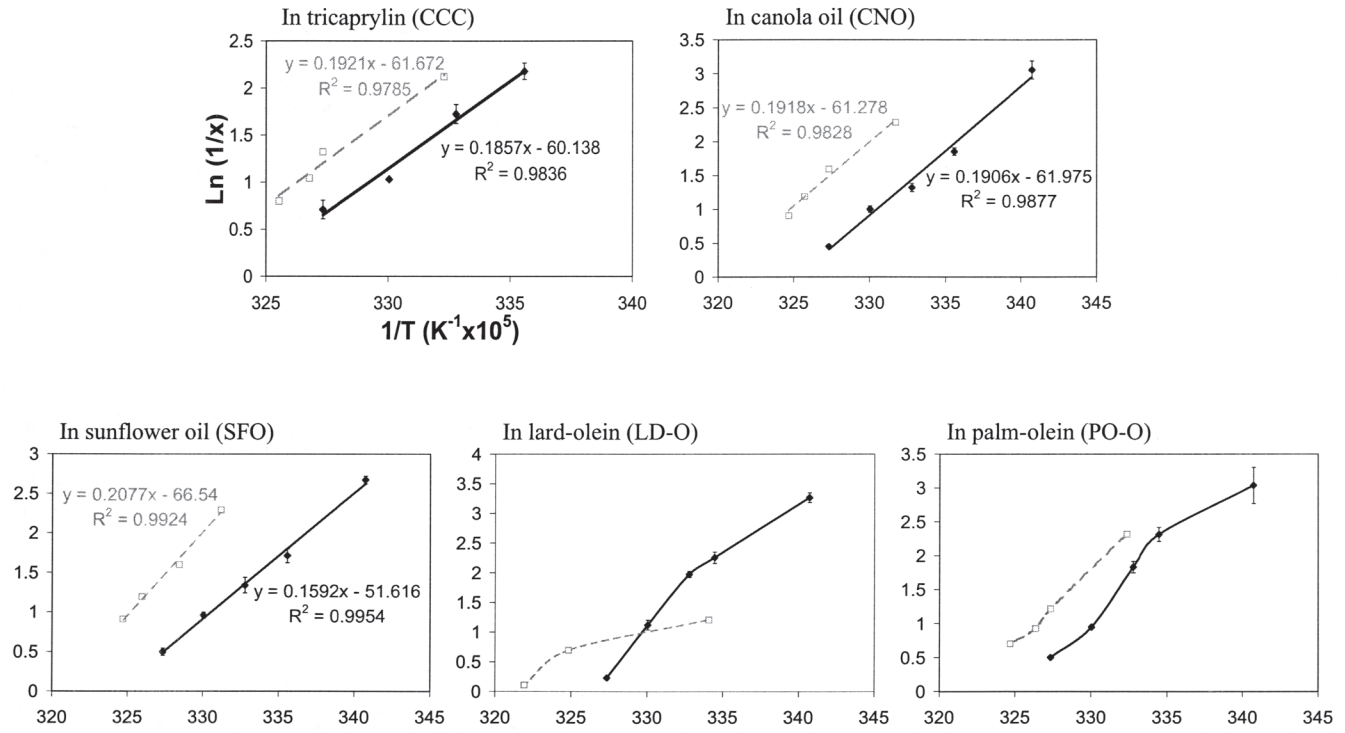

FIG. 3. Solubility curve (*x*, mole fraction) of cocoa butter-stearin (CB-S) as measured by compositional analysis (◆, solid lines) and extrapolated 0% solid fat measured by NMR (□, dashed lines).

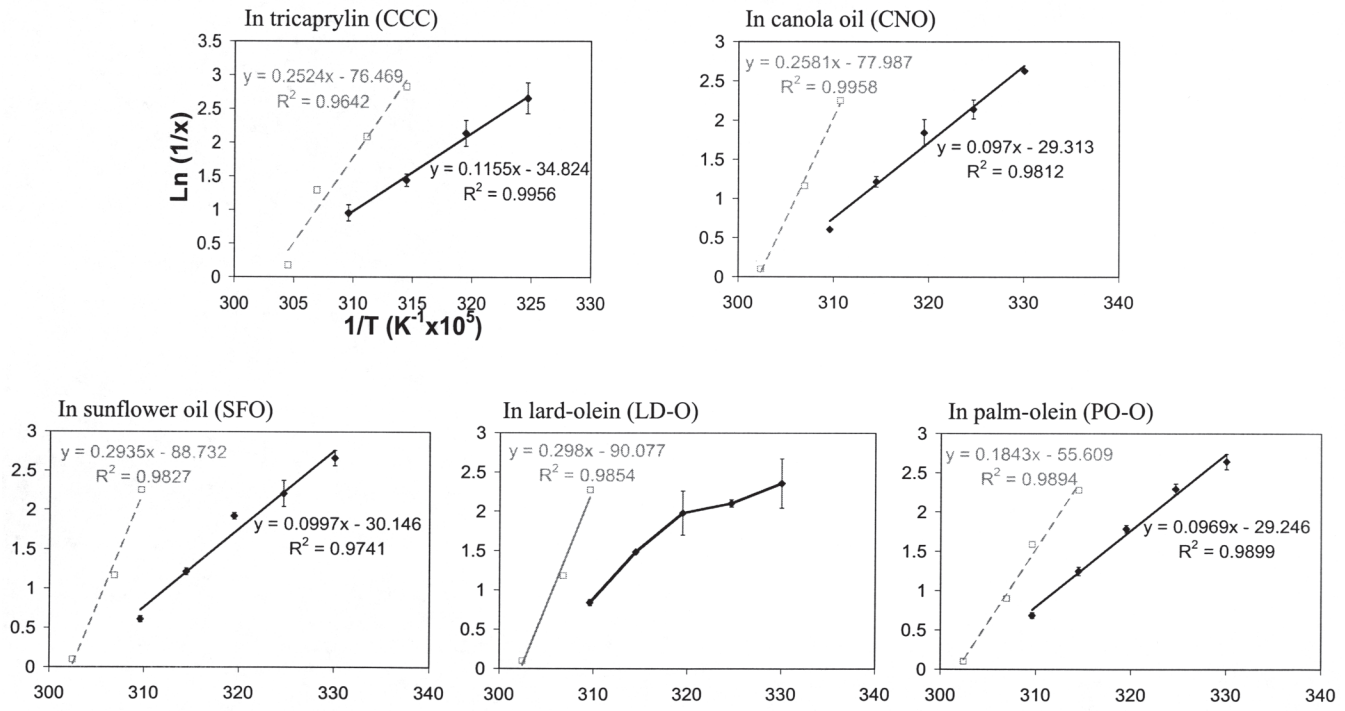

FIG. 4. Solubility curve (*x*, mole fraction) of palm oil-stearin (PO-S) as measured by compositional analysis (◆, solid lines) and extrapolated 0% solid fat measured by NMR (□, dashed lines).

these binary systems. On the other hand, the solubility of PO-S in CCC and LD-O was lower than the others when the temperature was higher than 45°C. The lower solubility resulted from the formation of a solid solution between PO-S and the low-melting fats (11).

SFC. The temperature at which each mixture had zero SFC was interpolated from the isosolids diagram. The comparison between the temperature at 0% SFC for each binary mixture of lipid classes and the solubility of the high-melting class in the low-melting fat is given in each of Figures 2–4. In general, this method gave lower solubility values than the compositional method.

Comparison of methods. Compositional analysis (analyzing the composition of high-melting fats dissolved in low-melting fats) allows construction of a partial solubility curve for a high-melting fat in liquid oil. The melting temperature and ΔH_{fus} calculated from the solubility curve can be compared with equilibrium results obtained from analyzing melting behavior of the pure fats, such as clear point determination and latent heat measurement by calorimetry.

The melting temperature and ΔH_{fus} of the high-melting fats were calculated from the linear relationship between ln x and $1/T$ for those low-melting fats in which ideal behavior was observed (Table 3). In general, the calculated results are similar to those determined by DSC (Table 2). For PPP-S, the melting temperature was about 63.5°C and ΔH_{fus} was 161 kJ/mol. This compares with 63.4°C and 150.5 kJ/mol from DSC analysis. In this case, which is a very pure system, the Hildebrand equation gives a melting temperature similar to the peak temperature in the DSC. For CB-S, the calculated melting temperature and ΔH_{fus} were approximately 35°C and 130 kJ/mol, close to those of the stored CB-S sample as determined by DSC (Table 2). In this case, where there was a wider range of TAG present, the Hildebrand equation gave a melting temperature value between the onset and peak temperatures. As seen in Table 3, the calculated melting temperature and ΔH_{fus} for PO-S in CNO, SFO, and PO-O were about 58°C and 81 kJ/mol, respectively, compared with the end point temperature of 57.1°C and ΔH_{fus} of 73.9 kJ/mol determined from the DSC curve for the PO-S sample (Table 2). This variability in melting temperature between the compositional analysis approach and the DSC results may arise from the spread of melting temperatures due to multiple TAG in the sample.

In cases where ideal solutions were formed, values of T_m and ΔH_{fus} calculated from the Hildebrand equation were generally similar to those found from calorimetric analysis, documenting that the simpler calorimetric approach may be sufficient for identifying equilibrium conditions for these systems. However, errors due to the spread of melting temperatures from the mixed TAG in natural fats may lead to substantial errors in the actual equilibrium condition.

Significant deviations between the two approaches were found for nonideal systems. Nonideal behavior of high-melting fats in some low-melting fats may be explained by their TAG compositions. For example, CCC was found to form a solid solution with all the high-melting fats, even though there is greater molecular dissimilarity between CCC and these high-melting fats. In this case, because CCC had very short chains

TABLE 3
Melting Temperature and ΔH_{fus} of High Melting-Fats in Various Low-Melting Fats as Determined from the Hildebrand Equation for Data on Compositional Analysis of Equilibrium Concentration[a]

	Tripalmitin sample		Cocoa butter-stearin		Palm oil-stearin	
Low-melting fats	Melting temperature (°C)	ΔH_{fus} (kJ/mol)	Melting temperature (°C)	ΔH_{fus} (kJ/mol)	Melting temperature (°C)	ΔH_{fus} (kJ/mol)
Canola oil	63.5	159.1	35.3	133.4	57.9	80.6
Sunflower oil	63.5	158.4	35.4	128.6	57.7	82.9
Lard-olein fraction	63.4	165.4	N/A	N/A	N/A	N/A
Palm-olein fraction	63.6	165.9	N/A	N/A	58.3	80.6

[a]N/A, not available.

(C8:0), it could fit easily into the cavity in the crystal structure of high-melting fats. However, the deviation from ideality in the mixture of CB-S/LD-O or CB-S/PO-O was due to the formation of solid solution between POP in CB-S and OOP in LD-O or PO-O (12).

Figures 2–4 compare the solubility measurements from compositional analysis and the extrapolation of NMR data to 0% SFC. In all cases, equilibrium values from extrapolation of SFC data were 30–70% lower than those determined by the compositional analysis method. This may simply be due to the nature of the extrapolation to 0% SFC in the isosolids diagram calculation, or it may reflect a lack of equilibration. Regardless, it is clear that the errors associated with extrapolation of SFC to zero do not permit a good estimate of phase equilibrium in these lipid systems.

ACKNOWLEDGMENTS

This work was supported in part by research grants from the USDA. Thanks to Yuping Shi for performing fat fractionation and to Baoming Liang for providing valuable advice.

REFERENCES

1. Hartel, R.W., and K.E. Kaylegian, Advances in Milk Fat Fractionation, in *Crystallization Processes in Fats and Lipid Systems*, edited by N. Garti and K. Sato, Marcel Dekker, New York, 2001, pp. 381–427.
2. Hannewijk, J., A.J. Haighton, and P.W. Hendrikse, Dilatometry of Fats, in *Analysis and Characterization of Oils, Fats and Fat Products*, edited by H.A. Boekenoogen, Interscience, London, 1964, pp. 119–182.
3. Timms, R.E., The Solubility of Milk Fat, Fully Hardened Milk Fat and Milk Fat Hard Fraction in Liquid Oils, *Aust. J. Dairy Technol. 33*:130–135 (1978).
4. Deman, J.M., L. Deman, and B. Blackman, Melting-Point Determination of Fat Products, *J. Am. Oil Chem. Soc. 60*:91–94 (1983).
5. Hartel, R.W., *Crystallization in Foods*, Aspen, New York, 2001.
6. Wesdorp, L.H., Liquid-Multiple Solid Phase Equilibria in Fats: Theory and Experiments, Ph.D. Thesis, Delft University of Technology, The Netherlands, 1990.
7. Geeraert, E., and P. Sandra, Capillary GC of Triglycerides in Fats and Oils Using a High Temperature Phenylmethylsilicone Stationary Phase. Part II. The Analysis of Chocolate Fats, *J. Am. Oil Chem. Soc. 64*:100–105 (1987).
8. IUPAC, *Standard Methods for the Analysis of Oils, Fats and Derivatives*, 7th edn., Oxford,United Kingdom, 1987.
9. Timms, R.E., Computer Program to Construct Isosolid Diagrams for Fat Blends, *Chem. Ind. (London) 7*:257–258 (1979).
10. Timms, R.E., Program to Calculate and Plot Isosolid Diagrams, ver. 4, IBM Compatible/BASIC (1982).
11. Knoester, M., P. De Bruijne, and M. Van den Tempel, The Solid-Liquid Equilibrium of Binary Mixtures of Triglycerides with Palmitic and Stearic Chains, *Chem. Phys. Lipids9*:309–319 (1972).
12. Rossell, J.B, Phase Diagrams of Triglyceride Systems, *Adv. Lipid Res. 5*:353–408 (1967).

[Received December 19, 2005; accepted March 1, 2006]